

A solid-state ^{133}Cs nuclear magnetic resonance and X-ray crystallographic study of cesium complexes with macrocyclic ligands

Alan Wong, Simon Sham, Suning Wang, and Gang Wu

Abstract: We report solid-state NMR determination of the ^{133}Cs chemical shift anisotropy (CSA) for a series of cesium complexes with macrocyclic ligands. It was found that the isotropic ^{133}Cs chemical shifts are related to the number of oxygen atoms to which the Cs^+ ion is coordinated. The ^{133}Cs chemical shifts were found to correlate with average Cs—O distances. We also attempt to use the established correlation to deduce Cs^+ coordination environment for compounds with unknown structures. We also report the X-ray determination of the crystal structure for $\text{Cs}(\text{DB18C6})_2\text{SCN}\cdot 1/2\text{CH}_3\text{OH}\cdot 1/2\text{H}_2\text{O}$. The compound crystallizes in monoclinic, $a = 14.503(2)$, $b = 15.152(3)$, $c = 39.989(6)$ Å, $\beta = 90.796(8)^\circ$, space group $P2_1/c$, $Z = 8$. There are two independent molecules in the asymmetric unit cell where each of the two Cs^+ ions is coordinated to two DB18C6 ligand molecules forming a sandwich-type structure.

Key words: solid state NMR, alkali metal, ^{133}Cs chemical shift, macrocyclic ligand, crystal structure.

Résumé : On a mesuré l'anisotropie du déplacement chimique du ^{133}Cs dans les spectres RMN à l'état solide d'une série de complexes du césium avec des ligands macrocycliques. On a trouvé que les déplacements chimiques isotropes du ^{133}Cs sont reliés au nombre d'atomes d'oxygène formant une coordination avec le Cs^+ . On a trouvé qu'il existe une corrélation entre les déplacements chimiques du ^{133}Cs et les distances moyennes Cs—O. On a aussi essayé d'établir une corrélation qui permettrait de déduire l'environnement de coordination du Cs^+ dans des composés de structures inconnues. On a aussi déterminé la structure du $\text{Cs}(\text{DB18C6})_2\text{SCN}\cdot 1/2\text{CH}_3\text{OH}\cdot 1/2\text{H}_2\text{O}$ par diffraction des rayons X. Les cristaux sont monocliniques, groupe d'espace $P2_1/c$, avec $a = 14,503(2)$, $b = 15,152(3)$ et $c = 39,989(6)$ Å, $\beta = 90,796(8)^\circ$ et $Z = 8$. Il y a deux molécules indépendantes dans la maille élémentaire asymétrique dans laquelle chacun des deux ions Cs^+ est coordonné à deux molécules de ligand DB18C6 formant une structure de type sandwich.

Mots clés : RMN à l'état solide, métal alcalin, déplacement chimique du ^{133}Cs , ligand macrocyclique, structure cristalline.

Introduction

Since Pedersen's (1) first synthesis of macrocyclic polyethers, a large number of acyclic, cyclic, and bicyclic crown ethers containing oxygen, nitrogen, and sulfur donor atoms have been prepared and extensively investigated (2). In the past 20 years, alkali metal nuclear magnetic resonance (NMR) spectroscopy has served as a major technique for studying the cation-binding properties of these macrocyclic complexes in solutions; however, relatively few solid-state alkali metal NMR studies were reported in the literature (3, 4). The advantage of solid-state metal NMR is that the alkali metal ions under observation are usually located in a well-defined coordination environment. In contrast, alkali metal

ions often undergo rapid exchange between bound and free states in the liquid phase, resulting in averaged NMR parameters. Since a large number of alkali metal complexes have been characterized by X-ray diffraction studies, it is desirable to document NMR parameters for alkali metal ions in various ion-binding environments. In addition, solid-state NMR is capable of yielding the orientation dependence of NMR parameters. This information is usually unavailable from the solution NMR spectra because of the molecular tumbling motion.

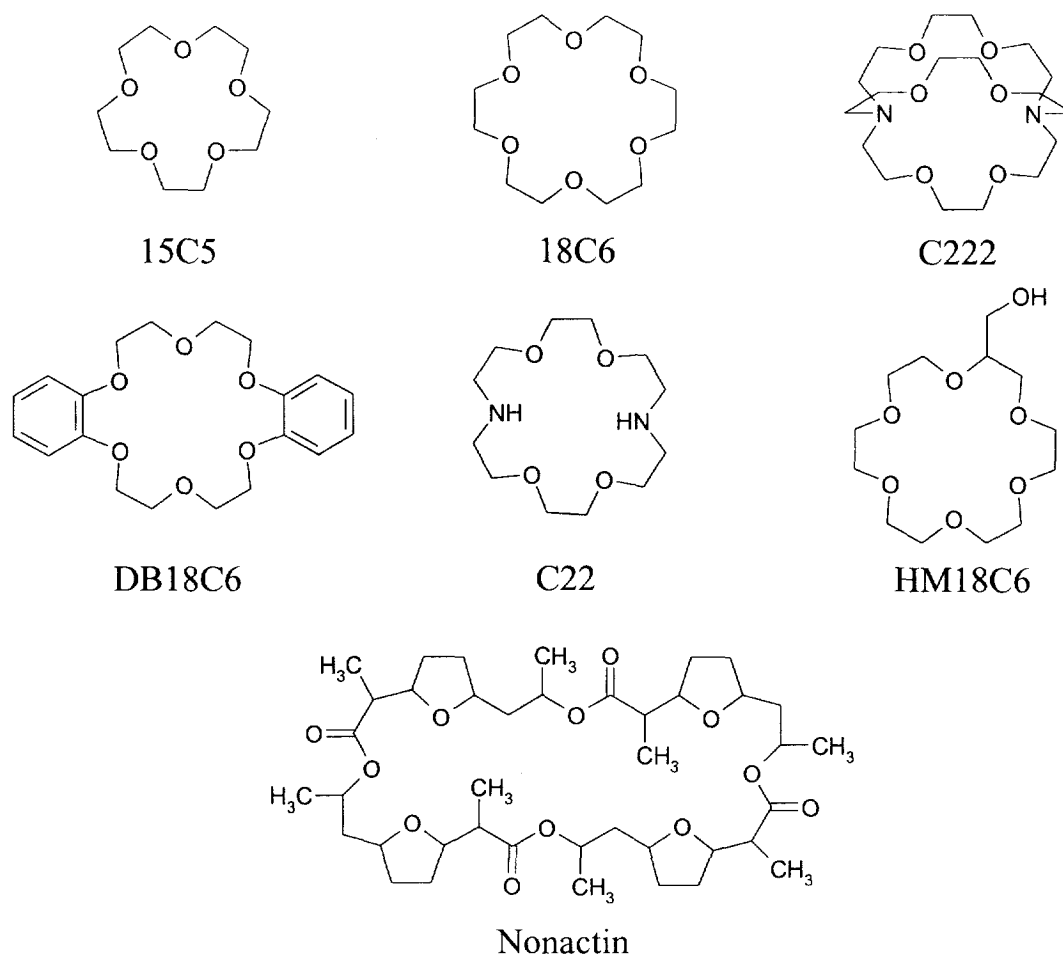
Cesium-133 is perhaps the easiest alkali metal nuclide for NMR measurements because of its favorable nuclear properties: 100% natural abundance, $I = 7/2$, and a small quadrupole moment of $Q = -3 \times 10^{-31} \text{ m}^2$. There have been several recent reports on the determination of ^{133}Cs chemical shift anisotropy (CSA) in simple inorganic salts (5–10); however, relatively little is known about solid-state ^{133}Cs NMR data for cesium macrocyclic complexes, except for solid alkali metal and electrides studied by Dye and co-workers (11–14). In this contribution, we report the determination of ^{133}Cs CSAs in a number of cesium macrocyclic compounds (Scheme 1). These complexes are used as models for establishing correlation between solid-state ^{133}Cs NMR parameters and Cs^+

Received January 14, 2000. Published on the NRC Research Press website on July 7, 2000.

A. Wong, S. Sham, S. Wang, and G. Wu,¹ Department of Chemistry, Queen's University, Kingston, ON K7L 3N6, Canada.

¹Author to whom correspondence may be addressed.
Telephone: (613) 533-2644. Fax: (613) 533-6669.
e-mail: gangwu@chem.queensu.ca

Scheme 1.



binding environment. We also report the crystal structure for $\text{Cs}(\text{DB18C6})_2\text{SCN}$.

Experimental

Materials

Cesium thiocyanate, cesium chloride, and macrocyclic ligands were purchased from Aldrich and used without further purification. All complexes were prepared according to the literature methods (15). In general, ligand and cesium salt are mixed in a suitable molar ratio in various solvents (methanol, ethanol, or acetone) and crystallized at either room temperature or 5°C. The melting points of the compounds were consistent with the literature values: mp: 201–202°C for $\text{Cs}(18\text{C6})\text{SCN}$, 191–193°C for $\text{Cs}(18\text{C6})_2\text{SCN}$, 152–153°C for $\text{Cs}(\text{DB18C6})_2\text{SCN}$, 99–100°C for $\text{Cs}(\text{C22})\text{SCN}$, and 146–148°C for $\text{Cs}(\text{C22})\text{SCN}$. Nonactin (purchased from Sigma) was mixed with CsSCN in a molar ratio of 1:1.5 in methanol. Gramicidin D [Dubos] was purchased from Sigma (80% gramicidin A, 6% gramicidin B, and 14% gramicidin C). Gramicidin A (25 mg/mL) was crystallized at 5°C from 50 mM solution of CsCl in methanol.

X-ray diffraction analyses

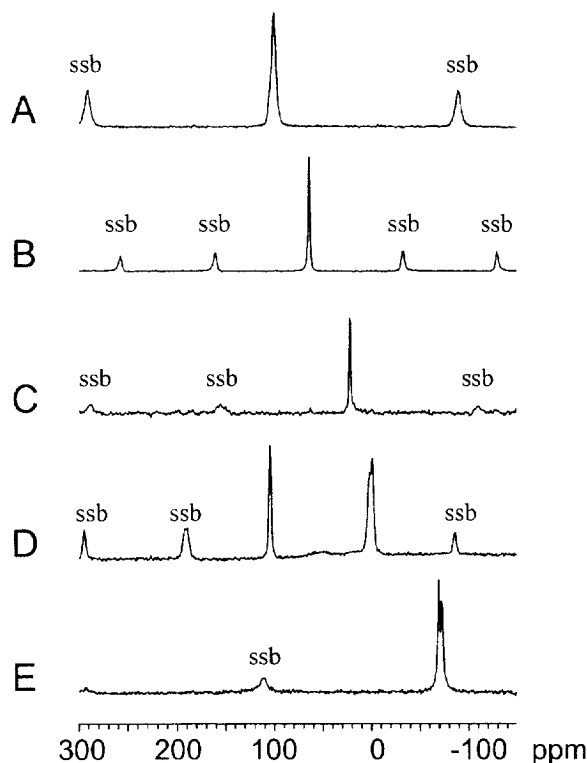
Large colorless crystals of $\text{Cs}(\text{DB18C6})_2\text{SCN}$ were prepared according to the procedure of Pederson (15) and

recrystallized twice from methanol. A crystal of size $0.2 \times 0.5 \times 0.4$ mm was sealed in a glass capillary. The X-ray data were collected on a Siemens P4 single-crystal diffractometer with graphite-monochromated $\text{Mo K}\alpha$ radiation, operated at 50 kV and 40 mA at 296 K. The data were collected over $\theta = 1.94$ – 22.51° . Data were processed on a Pentium PC using Siemens SHELXTL software package (16) and corrected for Lorentz and polarization effects.

Solid-state ^{133}Cs NMR

Solid-state ^{133}Cs NMR spectra were obtained on two spectrometers: Tecmag Apollo-200 (4.7 T, 26.32 MHz for ^{133}Cs) and Bruker Avance – 500 (11.7 T, 65.59 MHz for ^{133}Cs). Typical MAS frequencies were 5–12.5 kHz with Bruker 4 mm MAS probes. In MAS and central-transition static experiments, a single pulse sequence was used with pulse width of 1 μs (approx. 30° for the central transition). For the satellite-transition static experiments, a Hahn echo sequence was used to avoid acoustic ringing from the probe. Recycle times of 10–30 s were used. All ^{133}Cs chemical shifts were referenced to 0.5 M CsCl (aq.), $\delta = 0$ ppm, by setting the ^{133}Cs NMR signal of solid CsCl to $\delta = 223.2$ ppm. Spectral simulation was performed with the WSOLIDS program provided by Drs. Klaus Eichele and Rod Wasylshen (Dalhousie University, Halifax, Nova Scotia, Canada).

Fig. 1. Experimental ^{133}Cs MAS NMR spectra (11.75 T) of (a) $\text{Cs}(\text{C22})\text{SCN}$, (b) $\text{Cs}(\text{18C6})\text{SCN}$, (c) $\text{Cs}(\text{15C5})_2\text{SCN}$, (d) $\text{Cs}(\text{nonactin})\text{SCN}$, (e) $\text{Cs}(\text{DB18C6})_2\text{SCN}$.



Results and discussion

A. MAS ^{133}Cs NMR spectra

Solid-state ^{133}Cs NMR spectra obtained under the MAS condition are shown in Fig. 1. Since the ^{133}Cs nucleus has a very small quadrupole moment, no second-order quadrupolar broadening was observed at 11.75 T for the compounds studied in the present work. As shown in Fig. 1, each of the ^{133}Cs MAS spectra exhibits sharp isotropic peaks flanked by a large number of spinning sidebands due to the first-order quadrupole interaction. The Cs^+ ion in $\text{Cs}(\text{C22})\text{SCN}$ exhibits the least chemical shielding, $\delta_{\text{iso}} = 100$ ppm. The isotropic ^{133}Cs chemical shift for $\text{Cs}(\text{18C6})\text{SCN}$ is 64 ppm, which is quite different from the value of 73 ppm reported by Dye and coworkers (11). The reason for this discrepancy is unclear at this time. For the sandwich-type complex, $\text{Cs}(\text{15C5})_2\text{SCN}$, the Cs^+ ion shows more shielded environment, $\delta_{\text{iso}} = 22$ ppm. This chemical shift value is very similar to those found in alkalides, $\text{Cs}(\text{15C5})_2\text{M}^-$ ($\text{M} = \text{Na}, \text{K}, \text{Rb}$) (12), suggesting that the Cs^+ cation is well shielded by the two 15C5 ligands. For the Cs^+ -nonactin complex, the isotropic peak appears at 4 ppm and exhibits some broadening or splitting. Note that the sharp signal at 110 ppm is due to the excessive CsSCN in the sample. The ^{133}Cs NMR experiments performed at a different magnetic field (4.7 T) indicated that the broadening or splitting arises from a chemical shift distribution rather than from the second-order quadrupole interaction. Since the sample was prepared by lyophilizing a mixture containing excessive CsSCN ligand, it is of poorly crystalline nature.

Consequently, the observed broadening or splitting may be attributed to either lack of crystallinity or presence of polymorphs. The ^{133}Cs MAS spectrum of $\text{Cs}(\text{18C6})_2\text{SCN}$ exhibits a sharp peak at -72 ppm, which is dramatically different from that for $\text{Cs}(\text{18C6})\text{SCN}$, 64 ppm. The structure of $\text{Cs}(\text{18C6})_2\text{SCN}$ was speculated by Pedersen (15) to have a sandwich-type structure. The observation of a ^{133}Cs chemical shift of -72 ppm strongly supports the sandwich structure. Two sharp peaks were observed in the multiple-field ^{133}Cs MAS spectra of $\text{Cs}(\text{DB18C6})_2\text{SCN}$, $\delta_{\text{iso}} = -70$ and -72 ppm, indicating the presence of two crystallographically distinct Cs sites. Since the crystal structure of $\text{Cs}(\text{DB18C6})_2\text{SCN}$ has not been reported in the literature, we decided to carry out an X-ray single crystal diffraction study for this compound.

B. Crystal structure of $\text{Cs}(\text{DB18C6})_2\text{SCN}$

The crystal structure of $\text{Cs}(\text{DB18C6})_2\text{SCN}$ indicated the presence of two solvent molecules, thus the complete formula is $\text{Cs}(\text{DB18C6})_2\text{SCN} \cdot 1/2\text{CH}_3\text{OH} \cdot 1/2\text{H}_2\text{O}$. The crystal data are summarized in Table 1. The atomic coordinates with their estimated standard deviations are given in Table 2. Selected bond lengths and bond angles are listed in Table 3. As shown in Fig. 2, there are two molecules in the asymmetric unit cell, giving rise to two crystallographically inequivalent Cs sites. This finding is consistent with the observation of two chemical shifts in the ^{133}Cs MAS spectra. Each cesium ion is coordinated to twelve ether oxygen atoms from the two DB18C6 molecules, forming a hexagonal *anti*-prism coordination geometry around the Cs^+ ion. The Cs—O distances range from 3.188 to 3.586 Å for one site and from 3.206 to 3.787 Å for the other. The planes of the sandwiched cesium complex are approximately perpendicular to one another. The disordered counter ion (SCN^-), and both of the solvent molecules are not in direct contact with the central cesium ion. Interestingly, the crystal structure of $\text{Cs}(\text{DB18C6})_2\text{SCN}$ is very different from that of a closely related compound, $\text{Cs}(\text{tetramethyl-DB18C6})_2\text{SCN}$. The crystals of $\text{Cs}(\text{tetramethyl-DB18C6})_2\text{SCN}$ are tetragonal with space group of $P4_2/n$ (17). The asymmetric unit cell contains only one dimeric complex. Therefore, one isotropic ^{133}Cs chemical shift would be observed for this complex. The two ligand molecules lie on crystallographic two-fold axis giving rise to the $\bar{4}$ symmetry at the Cs^+ site. The three independent Cs—O distances in $\text{Cs}(\text{tetramethyl-DB18C6})_2\text{SCN}$, 3.12, 3.27, and 3.36 Å, are much shorter than those in $\text{Cs}(\text{DB18C6})_2\text{SCN}$.

C. Stationary ^{133}Cs NMR spectra

In order to obtain ^{133}Cs CSAs for the macrocyclic Cs complexes, it is necessary to obtain NMR spectra for stationary powder samples. The stationary ^{133}Cs NMR spectra are shown in Fig. 3. Since the ^{133}Cs second-order quadrupolar broadening is expected to be negligible (*vide infra*), it is straightforward to analyze the stationary ^{133}Cs NMR line shapes. In general, the ^{133}Cs CSAs for the macrocyclic polyether compounds are quite small, ranging from 50 to 90 ppm. However, a cryptand complex, $\text{Cs}(\text{C22})\text{SCN}$ exhibits a uniquely large CSA, 208 ppm. It is noted that similarly large ^{133}Cs CSAs have been previously observed in simple inorganic Cs salts. For example, the ^{133}Cs CSAs for the two

Table 1. Crystal data and structure refinement.

Empirical formula	C ₄₁ H ₄₈ CsNO ₁₂ S / 0.5CH ₃ OH / 0.5H ₂ O
Formula weight	936.3
Temperature	296(2) K
Wavelength	0.71073 Å
Crystal system	Monoclinic
Space group	<i>P</i> 2 ₁ / <i>c</i>
Unit cell dimensions	<i>a</i> = 14.503(2) Å <i>α</i> = 90° <i>b</i> = 15.152(3) Å <i>β</i> = 90.796(8)° <i>c</i> = 39.989(6) Å <i>γ</i> = 90°
Volume, <i>Z</i>	8787(2) Å ³ , 8
Density (calculated)	1.416 g/cm ³
Absorption coefficient	9.53 cm ⁻¹
<i>F</i> (000)	3852
Crystal size	0.2 × 0.5 × 0.4 mm
<i>θ</i> range for data collection	1.94 to 22.51°
Limiting indices	0 ≤ <i>h</i> ≤ 14, -16 ≤ <i>k</i> ≤ 0, -43 ≤ <i>l</i> ≤ 43
Reflections collected	11516
Independent reflections	10999 [<i>R</i> (int) = 0.0344]
Absorption correction	None
Refinement method	Full-matrix least-squares on <i>F</i> ²
Data / restraints / parameters	10656 / 0 / 1060
Goodness-of-fit on <i>F</i> ²	1.129
Final <i>R</i> indices [<i>I</i> > 2σ(<i>I</i>)]	<i>R</i> ₁ ^{<i>a</i>} = 0.0771, <i>wR</i> ₂ ^{<i>b</i>} = 0.1981
<i>R</i> indices (all data)	<i>R</i> ₁ ^{<i>a</i>} = 0.1198, <i>wR</i> ₂ ^{<i>b</i>} = 0.4128
Largest diff. peak and hole	0.855 and -1.180 eÅ ⁻³

$$^a R_1 = \frac{\sum |F_o| - |F_c|}{\sum |F_o|}$$

$$^b wR_2 = \left[\frac{\sum w[(F_o^2 - F_c^2)^2]}{\sum w(F_o^2)^2} \right]^{0.5} \text{ where } w = 1/[\sigma^2(F_o^2) + (0.075P)^2], \text{ where } P = [\max(F_o^2, 0) + 2F_c^2]/3$$

Table 2. Atomic coordinates (× 10⁴) and equivalent isotropic displacement parameters (Å² × 10³). *U*(eq) is defined as one third of the trace of the orthogonalized *U*_{ij} tensor.

	<i>x</i>	<i>y</i>	<i>z</i>	<i>U</i> (eq)
N(1)	-1658(13)	4539(18)	-2496(5)	175(9)
S(1)	3358(12)	6030(7)	116(3)	195(6)
Cs(1)	2147(1)	1050(1)	576(1)	61(1)
C(1)	895(8)	-758(7)	1143(3)	64(3)
O(1)	37(5)	167(5)	790(2)	68(2)
Cs(2)	3438(1)	4007(1)	-1777(1)	64(1)
S(2)	-2355(4)	4008(3)	-3078(2)	123(2)
N(2)	1660(35)	6556(26)	-57(14)	154(19)
C(2)	1077(9)	-1114(9)	1467(3)	76(4)
O(2)	72(5)	1341(5)	241(2)	74(2)
N(2A)	2266(31)	5959(29)	772(20)	241(39)
O(3)	1535(6)	1222(5)	-227(2)	73(2)
C(3)	557(11)	-849(11)	1727(4)	94(5)
O(4)	2890(5)	149(5)	-134(2)	64(2)
C(4)	-137(10)	-251(10)	1686(4)	83(4)
O(5)	2906(5)	-981(5)	436(2)	64(2)
C(5)	-328(8)	100(8)	1387(4)	75(4)
O(6)	1354(5)	-956(5)	862(2)	68(2)
C(6)	169(7)	-152(8)	1099(3)	59(3)
O(7)	3001(6)	676(6)	1311(3)	81(3)
C(7)	-663(9)	818(9)	740(4)	83(4)
O(8)	1647(5)	1992(5)	1310(2)	67(2)
C(8)	-750(9)	994(9)	383(4)	88(4)
O(9)	1521(5)	3049(5)	810(2)	73(2)
C(9)	-66(10)	1435(11)	-106(4)	95(5)
C(10)	768(11)	1820(10)	-261(4)	102(5)

Table 2 (Continued).

	<i>x</i>	<i>y</i>	<i>z</i>	<i>U</i> (eq)
O(10)	2793(6)	2929(6)	295(2)	85(3)
O(11)	4513(7)	2040(6)	447(3)	87(3)
C(11)	2315(9)	1427(8)	-402(3)	69(3)
C(12)	2420(11)	2124(9)	-609(4)	83(4)
O(12)	4476(7)	720(6)	840(3)	99(3)
C(13)	3218(15)	2256(10)	-772(4)	106(5)
O(13)	2676(6)	4702(6)	-1004(3)	94(3)
O(14)	4579(6)	4440(7)	-1109(3)	93(3)
C(14)	3954(12)	1703(10)	-725(4)	100(5)
C(15)	3874(10)	991(8)	-515(3)	78(4)
O(15)	5147(6)	2829(5)	-1366(2)	77(2)
O(16)	3942(6)	1836(6)	-1633(3)	87(3)
C(16)	3053(9)	838(7)	-356(3)	60(3)
C(17)	3662(8)	-379(8)	-38(4)	76(4)
O(17)	2113(6)	2292(6)	-1622(3)	94(3)
O(18)	1442(7)	3928(6)	-1365(3)	94(3)
C(18)	3332(9)	-1186(7)	130(3)	68(3)
C(19)	2504(9)	-1765(8)	573(4)	76(4)
O(19)	3004(6)	3173(6)	-2542(2)	89(3)
C(20)	2098(8)	-1586(7)	897(4)	74(4)
O(20)	1835(7)	4392(9)	-2452(3)	123(4)
O(21)	2273(6)	5787(7)	-2020(3)	112(4)
C(21)	809(8)	2413(8)	1273(3)	64(3)
O(22)	4118(6)	6108(5)	-1853(2)	81(3)
C(22)	75(10)	2330(9)	1483(4)	88(4)
O(23)	5383(5)	5048(5)	-2044(3)	82(3)

Table 2 (Continued).

	x	y	z	U(eq)
C(23)	-745(11)	2787(12)	1413(5)	109(6)
O(24)	4874(5)	3488(5)	-2388(2)	70(2)
C(24)	-802(11)	3330(11)	1155(5)	107(6)
C(25)	-54(11)	3451(9)	947(5)	98(5)
O(25)	891(17)	-5302(22)	1691(8)	303(14)
C(26)	764(9)	2992(8)	1005(4)	77(4)
C(27)	1537(10)	3666(9)	540(4)	86(4)
C(28)	2494(10)	3740(8)	428(4)	79(4)
C(29)	3607(12)	2922(11)	94(4)	106(5)
C(30)	4430(11)	2863(12)	260(5)	118(6)
O(30)	1842(11)	6419(11)	1316(5)	187(7)
C(31)	5290(10)	1929(8)	632(3)	71(3)
C(32)	6058(10)	2441(10)	610(4)	85(4)
C(33)	6803(12)	2283(13)	808(5)	103(5)
C(34)	6792(13)	1583(16)	1035(5)	116(6)
C(35)	6024(14)	1059(12)	1060(5)	112(6)
C(36)	5272(11)	1211(9)	849(4)	82(4)
C(37)	4291(13)	38(10)	1075(5)	114(6)
C(38)	3899(13)	321(15)	1363(6)	154(10)
C(39)	2729(10)	1123(10)	1613(4)	90(4)
C(40)	1764(9)	1405(8)	1585(3)	70(3)
C(41)	1228(10)	4081(9)	-1037(4)	77(4)
C(42)	379(11)	3832(10)	-905(5)	105(5)
C(43)	218(13)	4050(13)	-563(6)	120(7)
C(44)	872(15)	4440(14)	-379(5)	119(7)
C(45)	1706(12)	4675(11)	-510(5)	104(5)
C(46)	1880(11)	4484(9)	-841(4)	83(4)
C(47)	3426(14)	5033(16)	-800(6)	170(12)
C(48)	4181(14)	5110(15)	-911(7)	172(11)
C(49)	5275(11)	3955(10)	-948(4)	89(4)
C(50)	5771(9)	3417(9)	-1202(4)	80(4)
C(51)	5476(9)	2290(8)	-1602(3)	70(3)
C(52)	6383(9)	2250(9)	-1707(4)	77(4)
C(53)	6631(11)	1674(11)	-1954(4)	93(4)
C(54)	5989(12)	1160(10)	-2108(4)	94(5)
C(55)	5063(11)	1174(8)	-2004(4)	83(4)
C(56)	4821(9)	1740(8)	-1765(3)	68(3)
C(57)	3265(11)	1235(9)	-1745(4)	94(5)
C(58)	2407(11)	1408(10)	-1567(5)	112(6)
C(59)	1198(12)	2410(13)	-1496(6)	132(7)
C(60)	935(11)	3325(14)	-1577(6)	130(7)
C(61)	4946(8)	6225(7)	-1694(3)	58(3)
C(62)	5149(8)	6855(7)	-1447(3)	67(3)
C(63)	6029(10)	6891(9)	-1307(3)	79(4)
C(64)	6697(10)	6319(9)	-1404(4)	89(4)
C(65)	6507(8)	5691(8)	-1651(4)	73(4)
C(66)	5624(8)	5643(7)	-1790(3)	65(3)
C(67)	6047(8)	4444(9)	-2154(4)	76(4)
C(68)	5687(9)	3964(9)	-2442(4)	82(4)
C(69)	4561(9)	3029(10)	-2680(3)	79(4)
C(70)	3679(10)	2566(9)	-2618(4)	87(4)
C(71)	2098(9)	2907(11)	-2534(3)	81(4)
C(72)	1828(12)	2039(13)	-2566(4)	115(6)
C(73)	881(16)	1859(18)	-2545(6)	146(8)
C(74)	243(16)	2523(22)	-2515(7)	156(9)
C(75)	537(12)	3361(17)	-2490(4)	120(7)
C(76)	1480(10)	3585(13)	-2487(4)	95(5)

Table 2 (Concluded).

	x	y	z	U(eq)
C(77)	1290(14)	5183(18)	-2380(5)	165(11)
C(78)	1540(20)	5700(20)	-2216(12)	364(37)
C(79)	2699(11)	6612(10)	-2048(4)	92(5)
C(80)	3411(8)	6750(8)	-1785(3)	69(3)
C(81)	1218(19)	-4550(14)	1815(5)	157(9)
C(82A)	2501(41)	6013(22)	479(14)	156(35)
C(84)	-1959(13)	4301(13)	-2745(6)	109(6)
C(83A)	2284(46)	6304(27)	53(14)	138(20)
C(85)	5000	5000	0	312(40)

Table 3. Selected Cs—O bond lengths (Å) and O—Cs—O bond angles (°).

Cs(1)—O(10)	3.206(8)
Cs(1)—O(7)	3.225(9)
Cs(1)—O(9)	3.303(8)
Cs(1)—O(2)	3.307(8)
Cs(1)—O(5)	3.317(7)
Cs(1)—O(3)	3.330(9)
Cs(1)—O(4)	3.341(8)
Cs(1)—O(8)	3.352(8)
Cs(1)—O(6)	3.449(8)
Cs(1)—O(1)	3.459(8)
Cs(1)—O(12)	3.559(11)
Cs(1)—O(11)	3.787(9)
Cs(2)—O(14)	3.188(10)
Cs(2)—O(17)	3.295(9)
Cs(2)—O(21)	3.321(10)
Cs(2)—O(24)	3.326(8)
Cs(2)—O(22)	3.348(8)
Cs(2)—O(19)	3.361(9)
Cs(2)—O(18)	3.351(11)
Cs(2)—O(23)	3.417(8)
Cs(2)—O(16)	3.416(9)
Cs(2)—O(15)	3.452(9)
Cs(2)—O(13)	3.458(10)
Cs(2)—O(20)	3.586(12)
O(10)—Cs(1)—O(7)	111.4(2)
O(10)—Cs(1)—O(9)	50.7(2)
O(7)—Cs(1)—O(9)	90.3(2)
O(10)—Cs(1)—O(2)	90.5(2)
O(7)—Cs(1)—O(2)	136.8(2)
O(9)—Cs(1)—O(2)	74.9(2)
O(10)—Cs(1)—O(5)	131.7(2)
O(7)—Cs(1)—O(5)	82.4(2)
O(9)—Cs(1)—O(5)	172.7(2)
O(2)—Cs(1)—O(5)	110.9(2)
O(10)—Cs(1)—O(3)	70.6(2)
O(7)—Cs(1)—O(3)	170.7(2)
O(9)—Cs(1)—O(3)	97.5(2)
O(2)—Cs(1)—O(3)	50.9(2)
O(5)—Cs(1)—O(3)	89.7(2)
O(10)—Cs(1)—O(4)	88.1(2)
O(7)—Cs(1)—O(4)	125.3(2)
O(9)—Cs(1)—O(4)	135.2(2)

Table 3 (Continued).

O(2)-Cs(1)-O(4)	90.7(2)
O(5)-Cs(1)-O(4)	50.7(2)
O(3)-Cs(1)-O(4)	45.4(2)
O(10)-Cs(1)-O(8)	89.8(2)
O(7)-Cs(1)-O(8)	50.3(2)
O(9)-Cs(1)-O(8)	45.3(2)
O(2)-Cs(1)-O(8)	95.2(2)
O(5)-Cs(1)-O(8)	128.2(2)
O(3)-Cs(1)-O(8)	138.8(2)
O(4)-Cs(1)-O(8)	173.7(2)
O(10)-Cs(1)-O(6)	177.4(2)
O(7)-Cs(1)-O(6)	70.7(2)
O(9)-Cs(1)-O(6)	128.3(2)
O(2)-Cs(1)-O(6)	86.9(2)
O(5)-Cs(1)-O(6)	49.6(2)
O(3)-Cs(1)-O(6)	107.6(2)
O(4)-Cs(1)-O(6)	92.0(2)
O(8)-Cs(1)-O(6)	90.5(2)
O(10)-Cs(1)-O(1)	134.0(2)
O(7)-Cs(1)-O(1)	92.1(2)
O(9)-Cs(1)-O(1)	92.1(2)
O(2)-Cs(1)-O(1)	49.4(2)
O(5)-Cs(1)-O(1)	88.8(2)
O(3)-Cs(1)-O(1)	92.5(2)
O(4)-Cs(1)-O(1)	110.4(2)
O(8)-Cs(1)-O(1)	75.2(2)
O(6)-Cs(1)-O(1)	43.7(2)
O(10)-Cs(1)-O(12)	87.0(2)
O(7)-Cs(1)-O(12)	49.8(2)
O(9)-Cs(1)-O(12)	107.9(2)
O(2)-Cs(1)-O(12)	173.3(2)
O(5)-Cs(1)-O(12)	66.7(2)
O(3)-Cs(1)-O(12)	122.4(2)
O(4)-Cs(1)-O(12)	83.0(2)
O(8)-Cs(1)-O(12)	90.9(2)
O(6)-Cs(1)-O(12)	95.6(2)
O(1)-Cs(1)-O(12)	135.4(2)
O(10)-Cs(1)-O(11)	48.0(2)
O(7)-Cs(1)-O(11)	81.8(2)
O(9)-Cs(1)-O(11)	85.9(2)
O(2)-Cs(1)-O(11)	135.4(2)
O(5)-Cs(1)-O(11)	92.4(2)
O(3)-Cs(1)-O(11)	93.8(2)
O(4)-Cs(1)-O(11)	75.1(2)
O(8)-Cs(1)-O(11)	99.1(2)
O(6)-Cs(1)-O(11)	134.5(2)
O(1)-Cs(1)-O(11)	173.5(2)
O(12)-Cs(1)-O(11)	40.4(2)
O(14)-Cs(2)-O(17)	107.6(3)
O(14)-Cs(2)-O(21)	109.5(3)
O(17)-Cs(2)-O(21)	113.6(3)
O(14)-Cs(2)-O(24)	109.9(2)
O(17)-Cs(2)-O(24)	108.9(2)
O(21)-Cs(2)-O(24)	107.3(3)
O(14)-Cs(2)-O(22)	74.4(2)
O(17)-Cs(2)-O(22)	160.1(2)
O(21)-Cs(2)-O(22)	49.5(2)

Table 3 (Concluded).

O(24)-Cs(2)-O(22)	88.3(2)
O(14)-Cs(2)-O(19)	158.1(2)
O(17)-Cs(2)-O(19)	76.8(3)
O(21)-Cs(2)-O(19)	87.2(3)
O(24)-Cs(2)-O(19)	49.7(2)
O(22)-Cs(2)-O(19)	109.0(2)
O(14)-Cs(2)-O(18)	92.2(2)
O(17)-Cs(2)-O(18)	50.9(2)
O(21)-Cs(2)-O(18)	74.5(3)
O(24)-Cs(2)-O(18)	154.9(2)
O(22)-Cs(2)-O(18)	109.6(2)
O(19)-Cs(2)-O(18)	106.3(2)
O(14)-Cs(2)-O(23)	75.3(2)
O(17)-Cs(2)-O(23)	155.4(2)
O(21)-Cs(2)-O(23)	87.2(2)
O(24)-Cs(2)-O(23)	49.6(2)
O(22)-Cs(2)-O(23)	44.5(2)
O(19)-Cs(2)-O(23)	91.9(2)
O(18)-Cs(2)-O(23)	153.2(2)
O(14)-Cs(2)-O(16)	87.1(2)
O(17)-Cs(2)-O(16)	48.2(2)
O(21)-Cs(2)-O(16)	159.7(2)
O(24)-Cs(2)-O(16)	76.2(2)
O(22)-Cs(2)-O(16)	150.2(2)
O(19)-Cs(2)-O(16)	80.1(2)
O(18)-Cs(2)-O(16)	93.9(2)
O(23)-Cs(2)-O(16)	108.8(2)
O(14)-Cs(2)-O(15)	49.2(2)
O(17)-Cs(2)-O(15)	85.4(2)
O(21)-Cs(2)-O(15)	156.7(2)
O(24)-Cs(2)-O(15)	77.0(2)
O(22)-Cs(2)-O(15)	108.9(2)
O(19)-Cs(2)-O(15)	111.3(2)
O(18)-Cs(2)-O(15)	111.6(2)
O(23)-Cs(2)-O(15)	78.3(2)
O(16)-Cs(2)-O(15)	43.3(2)
O(14)-Cs(2)-O(13)	50.1(2)
O(17)-Cs(2)-O(13)	83.0(2)
O(21)-Cs(2)-O(13)	81.2(3)
O(24)-Cs(2)-O(13)	159.9(2)
O(22)-Cs(2)-O(13)	83.7(2)
O(19)-Cs(2)-O(13)	150.4(2)
O(18)-Cs(2)-O(13)	44.3(2)
O(23)-Cs(2)-O(13)	114.5(2)
O(16)-Cs(2)-O(13)	102.3(2)
O(15)-Cs(2)-O(13)	88.2(2)
O(14)-Cs(2)-O(20)	156.9(3)
O(17)-Cs(2)-O(20)	84.0(3)
O(21)-Cs(2)-O(20)	47.6(3)
O(24)-Cs(2)-O(20)	83.8(2)
O(22)-Cs(2)-O(20)	88.0(3)
O(19)-Cs(2)-O(20)	42.7(2)
O(18)-Cs(2)-O(20)	79.6(3)
O(23)-Cs(2)-O(20)	102.6(3)
O(16)-Cs(2)-O(20)	114.7(2)
O(15)-Cs(2)-O(20)	153.7(2)
O(13)-Cs(2)-O(20)	114.3(2)

Fig. 2. Diagram illustrating the two crystallographically inequivalent Cs sites in $\text{Cs}(\text{DB18C6})_2\text{SCN}\cdot\frac{1}{2}\text{CH}_3\text{OH}\cdot\frac{1}{2}\text{H}_2\text{O}$.

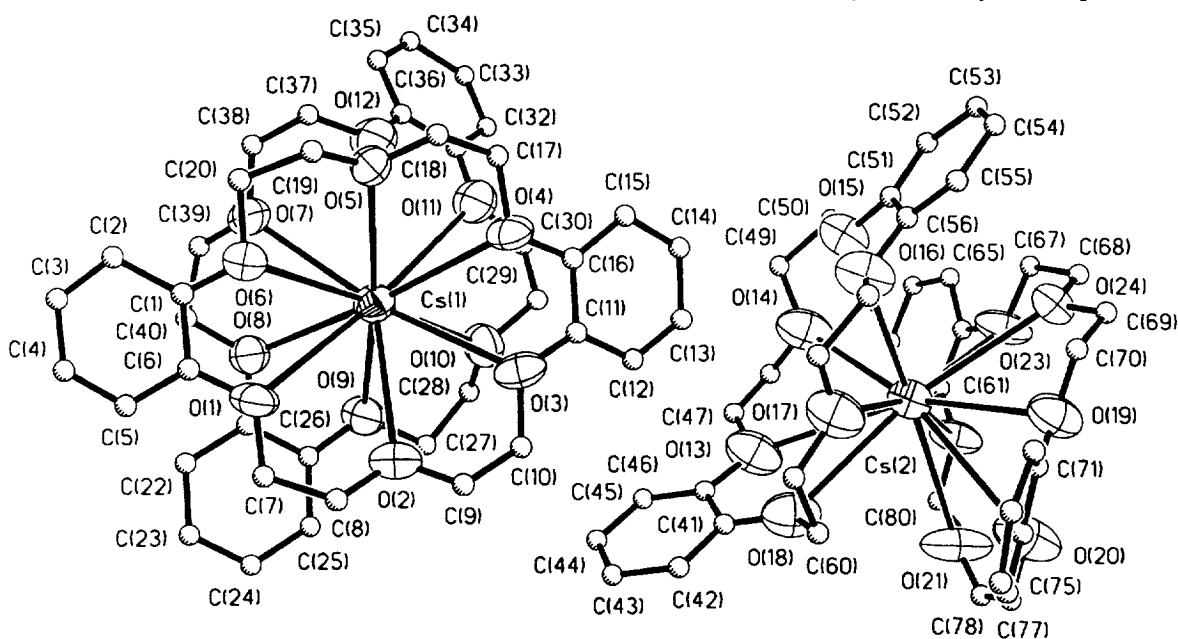
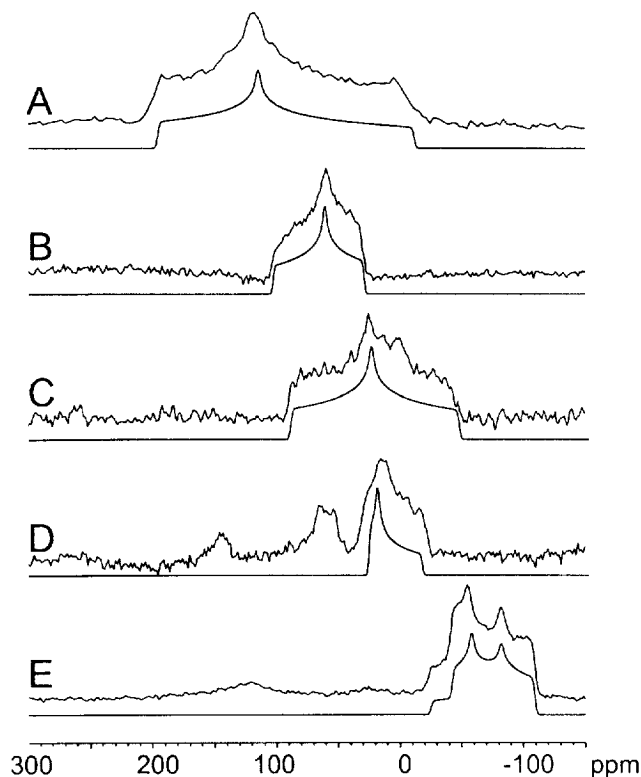


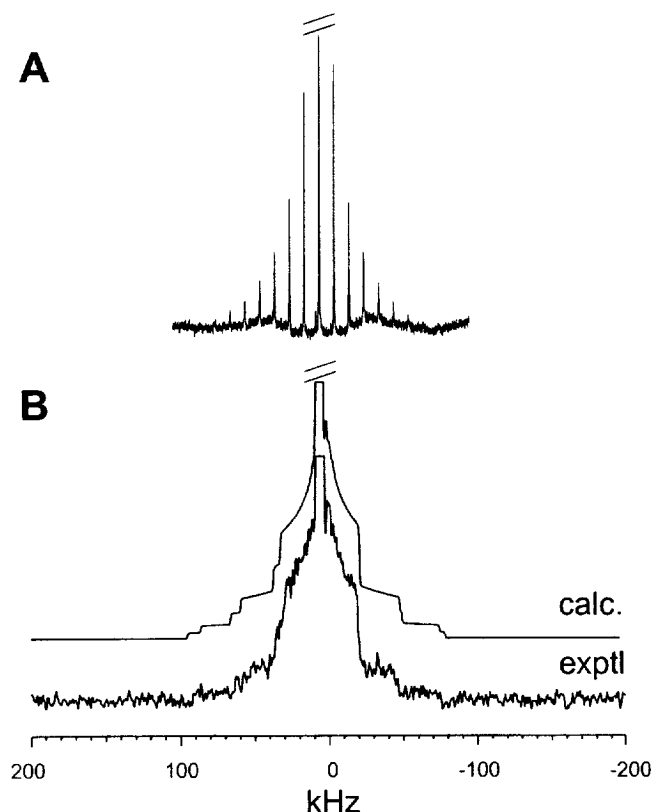
Fig. 3. Experimental (upper trace) and simulated (lower trace) central-transition ^{133}Cs stationary NMR spectra (11.75 T) of (a) $\text{Cs}(\text{C22})\text{SCN}$, (b) $\text{Cs}(\text{18C6})\text{SCN}$, (c) $\text{Cs}(\text{15C5})_2\text{SCN}$, (d) $\text{Cs}(\text{Nonactin})\text{SCN}$, and (e) $\text{Cs}(\text{DB18C6})_2\text{SCN}$.



Cs sites in Cs_2CrO_4 are 337 and 226 ppm (8). We also obtained the ^{133}Cs CSA for another cryptand complex, C222: $\delta_{11} = 251$, $\delta_{22} = 224$, and $\delta_{33} = 200$ ppm. The ^{133}Cs CSA for the Cs^+ -nonactin complex is also small. This is consistent with the crystal structure of $\text{CsSCN}/\text{nonactin}$ where the Cs^+ ion is located approximately at the center of a cube whose eight corners are formed by oxygen donor atoms from the

nonactin molecule (18). The stationary ^{133}Cs NMR spectrum of $\text{Cs}(\text{DB18C6})_2\text{SCN}$ exhibits a complex line shape due to the presence of two Cs sites. Since the isotropic chemical shifts have been determined from analysis of the MAS spectrum of $\text{Cs}(\text{DB18C6})_2\text{SCN}$, it is straightforward to analyze the stationary spectrum and obtain the principal components of the two ^{133}Cs CS tensors. The ^{133}Cs CSA results for the

Fig. 4. All-transition 10 kHz-MAS (a) and stationary (b) ^{133}Cs NMR spectra (11.75 T) of $\text{Cs}(\text{18C6})\text{SCN}$. The following parameters were used in the simulation shown in (b): $\delta_{11} = 103$, $\delta_{22} = 61$, and $\delta_{33} = 29$ ppm; $\text{QCC} = 0.41$ MHz; $\eta = 0.85$; $\alpha = 0$; $\beta = 80$; and $\gamma = 0^\circ$.

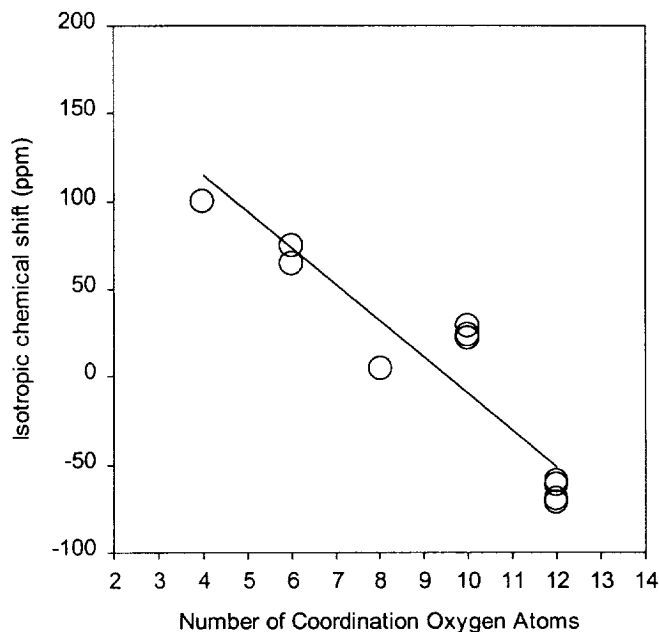


macrocyclic complexes are summarized in Table 4. However, it is also evident from Fig. 3 that some additional features are present in the ^{133}Cs stationary spectra. For example, a broad hump at 120 ppm was observed in the stationary spectrum of $\text{Cs}(\text{DB18C6})_2\text{SCN}$ (Fig. 3d). Since the ^{133}Cs MAS spectra of these complexes did not indicate any impurity, the low-intensity spectral features must arise from the satellite transitions. To obtain an estimate of the ^{133}Cs quadrupole coupling constant (QCC) for Cs-macrocyclic complexes, we recorded a complete stationary spectrum for $\text{Cs}(\text{18C6})\text{SCN}$, i.e., both central- and satellite transitions. As shown in Fig. 4, the all-transition ^{133}Cs NMR spectrum covers a range of approximately 200 kHz. Simulation yields that the ^{133}Cs QCC is 0.41 MHz and the asymmetry parameter is 0.85 for $\text{Cs}(\text{18C6})\text{SCN}$. At 11.75 T, the second-order ^{133}Cs quadrupolar interaction contributes less than 1 ppm to the stationary central-transition ^{133}Cs spectra and, consequently, can safely be ignored in the spectral analysis, confirming our previous assumptions. The ^{133}Cs MAS spectra of other Cs macrocyclic complexes exhibited similar spinning sideband manifold, suggesting that the QCCs are of similar magnitude as that for $\text{Cs}(\text{18C6})\text{SCN}$.

D. ^{133}Cs chemical shifts and ion-binding environment

The origin of ^{133}Cs chemical shielding (σ) can be written as a sum of two contributions (19):

Fig. 5. Correlation between the experimental ^{133}Cs isotropic chemical shift and the number of coordination oxygen atoms for cesium-macrocyclic compounds.

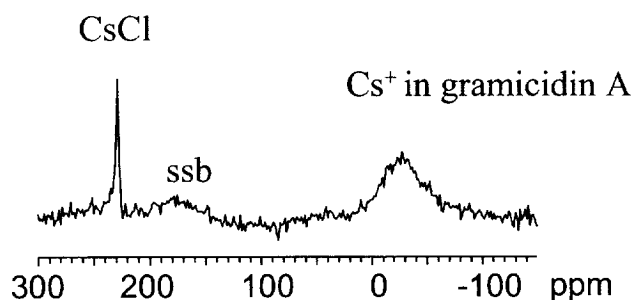


$$\sigma = \sigma_d + \sigma_p$$

where σ_d is the diamagnetic shielding term arising from the induced motion of a spherically symmetric electron cloud at a nucleus, and σ_p is the paramagnetic term caused by mixing of the electronic ground state with excited states in the presence of a strong external magnetic field. To a very crude approximation the paramagnetic shielding (σ_p) is proportional to $-(1/\Delta E) \langle 1/r^3 \rangle (\rho_e)$, where ΔE is the average energy separation between the ground and excited states of the molecule, $\langle 1/r^3 \rangle$ is the average distance between electrons and the nucleus of interest, and ρ_e is the relative electron densities in the various p orbitals involved in bonding (20-22). In the case of ^{133}Cs NMR, the paramagnetic term is usually a dominant contributor to variations of ^{133}Cs chemical shifts because of the relatively low energy gap (ΔE) and the availability of the outer p and d orbitals (23).

As shown in Fig. 5, the isotropic ^{133}Cs chemical shifts in macrocyclic compounds exhibit a clear correlation with the number of the oxygen atoms to which the Cs^+ ion is coordinated. It should be pointed out that for complexes with unknown crystal structures, all oxygen atoms in the macrocyclic ligand molecule were assumed to participate the interaction to the Cs^+ ion. Figure 5 suggests that, as the coordination number is increased, the chemical shielded at the Cs center is also increased. A similar correlation has also been observed between the Gutmann donor number (24) of the solvent and NMR chemical shifts of ^{23}Na (25, 26), ^{133}Cs (27), and ^{39}K (28) nuclei. The range of the ^{133}Cs chemical shifts plotted in Fig. 5, 100 ppm to -71 ppm, covers approximately the entire ^{133}Cs chemical shift range for Cs compounds containing oxygen ligands. However, one notable exception is the isotropic ^{133}Cs chemical shift for $\text{Cs}(\text{C222})\text{SCN}$, $\delta_{\text{iso}} = 225$ ppm. The cage structure of the C222 molecule forces very close contacts between the Cs^+

Fig. 6. Central-transition ^{133}Cs MAS spectrum (11.75 T) of gramicidin A/CsCl.

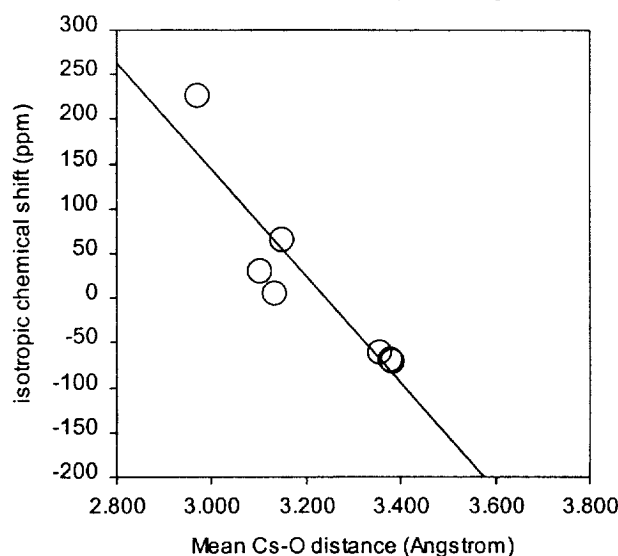


ion and the six oxygen donor atoms, with the average Cs—O distance of 2.970 Å (29). This strong Cs—O overlap is responsible for the unusually large chemical shift in Cs(C22)SCN (*vide infra*).

Ideally, one would use such a linear correlation to predict Cs^+ binding environments for compounds whose crystal structures are unknown. To test this idea, we obtained the solid-state ^{133}Cs NMR spectra for Cs(HM18C6)SCN· $x\text{H}_2\text{O}$. The isotropic ^{133}Cs chemical shift for this compound was found to be 0 ppm. Using the correlation curve shown in Fig. 5, we may predict that the Cs^+ ion in Cs(HM18C6)SCN· $x\text{H}_2\text{O}$ is probably coordinated to approximately nine or ten oxygen atoms. This indicates that, in addition to the six oxygen atoms from the 18C6 ring, the hydroxyl side-arm must also be bound to the Cs^+ ion, presumably in a similar fashion as those in sodium and potassium complexes of 16-(2-hydroxyethyl)-1,4,7,10,13-pentaoxa-16-azacyclooctadecane (30). The additional oxygen donors may come from water molecules. It is known that hydration water molecules are also commonly found in metal macrocyclic complexes (30). Therefore, the observed ^{133}Cs isotropic chemical shift of Cs(HM18C6)SCN· $x\text{H}_2\text{O}$ can be rationalized by a Cs^+ ion-binding environment containing nine or ten Cs—O interactions.

A crystalline sample of gramicidin A/CsCl complex was also prepared with the expectation that solid-state ^{133}Cs NMR may shed some light on the Cs^+ binding geometry inside the ion channel. The unit cell dimensions determined for our crystals are 35.565, 35.565, and 62.086 Å with the space group of $P4222$. However, these crystal data are different from all available crystal structures for gramicidin A/CsCl system (31–35). Clearly, our gramicidin A/CsCl crystals represented a new polymorph. Unfortunately, attempts to find the solution of the crystal structure for our gramicidin A/CsCl crystals were unsuccessful. Nevertheless, we obtained the ^{133}Cs MAS NMR spectrum for this crystalline sample. As shown in Fig. 6, a broad peak at 17 ppm is observed in the ^{133}Cs MAS spectrum. The line width of the broad peak is approximately 3.3 kHz. The broadening may be due to the presence of multiple Cs sites in the gramicidin A channel formed by a gramicidin dimer and likely the presence of two independent dimers in the asymmetric unit cell (31–35). In addition, it is also likely that, for each Cs^+ site, there exists a distribution of ^{133}Cs chemical shifts due to the presence of disorder. According to the correlation shown in Fig. 5, the ^{133}Cs chemical shift value of 17 ppm indicates the number of oxygen coordination at the binding sites is ap-

Fig. 7. Correlation between the ^{133}Cs chemical shifts and the average Cs—O distance for cesium-macrocyclic compounds.



proximately 8. This type of binding environment is consistent with those reported for other forms of gramicidin A crystals (31–36). For example, a recent X-ray study of gramicidin A/CsCl (36) revealed that two dimers are present in the asymmetric unit cell and that each gramicidin channel (dimer) contains three Cs^+ binding sites. On average, each Cs^+ ion has eight closest contacts arising from six carbonyl oxygens (3.6–4.5 Å) and two water oxygens (2.8–3.1 Å). Therefore, our solid-state ^{133}Cs NMR observation is in agreement with the crystallographic studies in the Cs^+ binding environment, despite the difference in overall crystal structures. It would be of interest to extend the alkali metal NMR to other gramicidin-cation complexes (Na and K).

In the above discussion, we have focused only on the isotropic ^{133}Cs chemical shifts. In the discussion that follows, we briefly comment on the observed tensor components for the Cs complexes with macrocyclic ligands. As seen from Table 4, the span of the chemical shift tensor varied from 26 ppm in Cs(18C6) $_2$ SCN to 208 ppm in Cs(C22)SCN. This large difference may be interpreted as due to the structural difference between the two complexes. Clearly, the Cs^+ coordination environment in Cs(18C6) $_2$ SCN is more “spherical” than that in Cs(C22)SCN. In principle, the tensor components are more informative than the isotropic value alone. However, for the ^{133}Cs NMR data presented in Table 4, there does not exist any clear trend between δ_{11} and δ_{33} components and ion-binding environment. Interestingly, the δ_{22} components show a nice correlation to the isotropic values. More studies are clearly required to unravel the relationship between individual chemical shift tensor components and ion coordination geometry.

In general, increasing the number of metal-ligand coordination also leads to an increase in the average metal-ligand distance. This is also true in the systems studied here. For example, the average Cs—O distance in Cs(18C6)SCN is 3.150 Å, which compares to 3.382 Å in Cs(DB18C6) $_2$ SCN. Dye and coworkers (12) suggested an inverse correlation between ^{133}Cs chemical shifts and the mean Cs—O distance. Figure 7 shows the ^{133}Cs isotropic chemical shift versus the

Table 4. Experimental ^{133}Cs NMR chemical shift tensors and structural data for the Cs macrocyclic complexes.

Compound	δ_{iso} (ppm)	δ_{11} (ppm)	δ_{22} (ppm)	δ_{33} (ppm)	Ω^a (ppm)	Coordination oxygen atom	Average $d(\text{Cs}\dots\text{O})$ (Å)	Range $d(\text{Cs}\dots\text{O})$ (Å)	NMR ref.
Cs(18C6)SCN	64	103	61	29	74	6	3.150 ^b	3.040–3.270	This work
Cs(18C6) ₂ SCN	-72	-61	-68	-87	26	12	—	—	This work
Cs(DB18C6) ₂ SCN (1)	-70	-42	-58	-109	67	12	3.386	3.206–3.787	This work
Cs(DB18C6) ₂ SCN (2)	-72	-25	-82	-109	84	12	3.377	3.188–3.586	This work
Cs(C22)SCN	100	196	115	-12	208	4	—	—	This work
Cs(Nonactin)SCN	4	27	10	-26	53	8	3.136 ^c	3.069–3.181	This work
Cs(15C5) ₂ SCN	22	90	25	-46	136	10	—	—	This work
Cs(HM18C6)SCN·xH ₂ O	0	38	-12	-26	64	—	—	—	This work
Cs(C222)SCN	225	251	224	200	51	—	2.970 ^d	2.960–2.970	This work
Cs(18C6) ₂ Na ⁻	-61	—	—	—	—	12	3.357 ^e	3.287–3.468	12
Cs(18C6) ₂ Cs ⁻	-61	—	—	—	—	12	3.31 ^f	3.113–3.516	11
Cs(15C5) ₂ Na ⁻	24	—	—	—	—	10	—	—	12
Cs(15C5) ₂ Rb ⁻	24	—	—	—	—	10	—	—	12
Cs(15C5) ₂ K ⁻	29	—	—	—	—	10	3.088 ^g	3.056–3.171	12
Cs(18C6)SCN	73	—	—	—	—	6	—	—	11
Cs(18C6) ₂ SCN	-59	—	—	—	—	12	—	—	11

^aSpan, = $\delta_{11} - \delta_{33}$.^bFrom ref. 38.^cFrom ref. 18.^dFrom ref. 29.^eFrom ref. 39.^fFrom ref. 12.^gFrom ref. 40.

average Cs—O distance for compounds with known crystal structures. Clearly, large ^{133}Cs chemical shifts are observed at short Cs—O distances. There also exist several examples in the literature where large ^{133}Cs chemical shift values were found for Cs sites exhibiting short Cs—O distances. Skibsted et al. (7) have observed a large ^{133}Cs chemical shift, 178 ppm, in Cs_2CO_3 for a site that is associated with a very short average Cs—O distance, 2.69 Å. Such a short Cs—O distance may allow an efficient electron transfer to occur from the donor oxygen atom in the ligand molecule to a $3p$ orbital of the metal ion (37), thus increasing the paramagnetic shielding contribution.

Conclusions

We have reported the determination of ^{133}Cs CSAs for a series of Cs complexes with macrocyclic molecules. The ^{133}Cs isotropic chemical shifts were found to exhibit a linear dependence on the number of oxygen atoms to which the Cs^+ ion is coordinated. In addition, the ^{133}Cs chemical shifts were also found to correlate with the average Cs—O distances. It would be of interest to find a general bonding parameter that can unify the two aforementioned dependencies. The established correlation may be useful in predicting Cs^+ ion-binding environment for unknown systems based on solid-state ^{133}Cs NMR data alone. We have also determined the crystal structure for $\text{Cs}(\text{DB18C6})_2\text{SCN}\cdot 1/2\text{CH}_3\text{OH}\cdot 1/2\text{H}_2\text{O}$.

Acknowledgments

This research was financially supported by grants from the Natural Sciences and Engineering Research Council (NSERC) of Canada. We wish to thank Mr. Chris Freure and

Dr. Shuan Dong for assistance in sample preparation and Dr. Zongchao Jia for the X-ray measurement of gramicidin A/CsCl crystals.

Supplementary material available

Anisotropic displacement parameters and hydrogen coordinates for $\text{Cs}(\text{DB18C6})_2\text{SCN}\cdot 1/2\text{CH}_3\text{OH}\cdot 1/2\text{H}_2\text{O}$ (5 pages) have been deposited as supplementary material and may be purchased from: The Depository of Unpublished Data, Document Delivery, CISTI, National Research Council Canada, Ottawa, Ontario, Canada, K1A 0S2.

References

1. C.J. Pedersen. *J. Am. Chem. Soc.* **89**, 7017 (1967).
2. (a) J.J. Christensen, D.J. Eatough, and R.M. Izatt. *Chem. Rev.* **74**, 351 (1974); (b) N.S. Poonia and A.V. Bajaj. *Chem. Rev.* **79**, 389 (1979).
3. C. Detellier, H.P. Graves, and K.M. Brière. *In Isotopes in physical and biomedical science. Edited by E. Buncler and J.R. Jones.* Elsevier Science Publications B.V., Amsterdam, 1991. Vol. 2, Chap. 4.
4. G.W. Buchanan. *Prog. Nucl. Magn. Reson. Spectrosc.* **34**, 327 (1999).
5. S. Mooibroek, R.E. Wasylshen, R. Dickson, and G. Facey. *J. Magn. Reson.* **66**, 542 (1986).
6. W.P. Power, R.E. Wasylshen, S. Mooibroek, B.A. Pettitt, and W. Danchura. *J. Phys. Chem.* **94**, 591 (1990).
7. S. Kroeker, K. Eichele, R.E. Wasylshen, and J.F. Britten. *J. Phys. Chem. B*, **101**, 3727 (1997).
8. W.P. Power, S. Mooibroek, R.E. Wasylshen, and T.S. Cameron. *J. Phys. Chem.* **98**, 1552 (1994).
9. J. Skibsted, T. Vosegaard, H. Bildsøe, and H.J. Jakobsen. *J. Phys. Chem.* **100**, 14872 (1996).

10. H. Honda, M. Kenmotsu, N.O. Yamamuro, H. Ohki, S. Ishimaru, R. Ikeda, and Y. Furukawa. *Z. Naturforsch. A: Phys. Sci.* **51a**, 761 (1996).
11. A. Ellaboudy, J.L. Dye, and P.B. Smith. *J. Am. Chem. Soc.* **105**, 6490 (1983).
12. R.H. Huang, D.L. Ward, M.E. Kuchenmeister, and J.L. Dye. *J. Am. Chem. Soc.* **109**, 5561 (1987).
13. M.J. Wagner, L.E.H. McMills, A. Ellaboudy, J.L. Eglin, J.L. Dye, P.P. Edwards, and N.C. Pyper. *J. Phys. Chem.* **96**, 9656 (1992).
14. A. Ellaboudy, M.L. Tinkham, B.V. Eck, and J.L. Dye. *J. Phys. Chem.* **88**, 3852 (1984).
15. C.J. Pedersen. *J. Am. Chem. Soc.* **92**, 386 (1970).
16. SHELXTL Crystal Structure Analysis Package; Version 5. Bruker Analytical X-ray System, Siemens, Madison, Wis. 1995.
17. P.R. Mallinson. *J. Chem. Soc. Perkin Trans. 2*, 261 (1975).
18. T. Sakamaki and Y. Iitaka. *Acta Crystallogr. Sect B: Struct. Crystallogr. Cryst. Chem.* **B33**, 52 (1977).
19. (a) N.F. Ramsey. *Phys. Rev.* **78**, 699 (1950); (b) **83**, 540 (1951); (c) **86**, 243 (1952).
20. M. Karplus and J.A. Pople. *J. Chem. Phys.* **38**, 2803 (1963).
21. C.J. Jameson and H.S. Gutowsky. *J. Chem. Phys.* **40**, 1714 (1964).
22. J.A. Pople. *Mol. Phys.* **7**, 301 (1964).
23. D.W. Hafemeister and W.A. Flygare. *J. Chem. Phys.* **44**, 3584 (1966).
24. V. Gutmann and W. Wychera. *Inorg. Nucl. Chem. Lett.* **2**, 257 (1966).
25. E.G. Bloor and R.G. Kidd. *Can. J. Chem.* **46**, 3425 (1968).
26. R.H. Erlich, E. Roach, and A.I. Popov. *J. Am. Chem. Soc.* **92**, 4989 (1970).
27. W.J. DeWitte, L. Liu, E. Mei, J.L. Dye, and A.I. Popov. *J. Solution. Chem.* **6**, 337 (1977).
28. J.S. Shih and A.I. Popov. *Inorg. Nucl. Chem. Lett.* **13**, 105 (1977).
29. P.D. Moras, B. Metz, and R. Weiss. *Acta Crystallogr. Sect B: Struct. Crystallogr. Cryst. Chem.* **B29**, 388 (1973).
30. F.R. Fronczek and R.D. Gandour. *In Cation binding by macrocycles*. Marcel New Dekker Inc., New York. 1990.
31. R.E. Koeppe, J.M. Berg, K.O. Hodgson, and L. Stryer. *Nature (London)*, **279**, 723 (1979).
32. B.A. Wallace and K. Ravikumar. *Science (Washington, D.C.)*, **241**, 182 (1988).
33. B.A. Wallace, W.A. Hendrickson, and K. Ravikumar. *Acta Crystallogr. Sect B: Struct. Crystallogr. Cryst. Chem.* **B46**, 440 (1990).
34. B.A. Wallace. *Progr. Biophys. Mol. Biol.* **57**, 59 (1992).
35. D.A. Doyle and B.A. Wallace. *J. Mol. Biol.* **266**, 963 (1997).
36. B.M. Burhart, N. Li, D.A. Langs, W.A. Pangborn, and W.L. Duax. *Proc. Natl. Acad. Sci. U.S.A.* **95**, 12950 (1998).
37. R. Tabeta, M. Aida, and H. Saito. *Bull. Chem. Soc. Jpn.* **59**, 1957 (1986).
38. M. Dobler and R.P. Phizackerley. *Acta Crystallogr. Sect B: Struct. Crystallogr. Cryst. Chem.* **B30**, 2748 (1974).
39. S.B. Dawes, D.L. Ward, O. Fussa-Rydell, R.H. Huang, and J.L. Dye. *Inorg. Chem.* **28**, 2132 (1989).
40. D.L. Ward, R.H. Huang, and J.L. Dye. *Acta Crystallogr. Sect C: Cryst. Struct. Commun.* **C46**, 1838 (1990).